Available online at www.sciencedirect.com
ScienceDirect
Bioorganic & Medicinal Chemistry Letters
Bioorganic & Medicinal Chemistry Letters 16 (2006) 5488–5492

3,4,5-Trisubstituted isoxazoles as novel PPARδ agonists. Part 2

Robert Epple,[a,*] Mihai Azimioara,[a] Ross Russo,[a] Yongping Xie,[a] Xing Wang,[a] Christopher Cow,[a] John Wityak,[a] Don Karanewsky,[a] Badry Bursulaya,[b] Andreas Kreusch,[b] Tove Tuntland,[c] Andrea Gerken,[c] Maya Iskandar,[c] Enrique Saez,[c] H. Martin Seidel[c] and Shin-Shay Tian[c]

[a]*Department of Medicinal Chemistry, The Genomics Institute of the Novartis Research Foundation, 10675 John Jay Hopkins Drive, San Diego, CA 92121, USA*
[b]*Department of Structural Biology, The Genomics Institute of the Novartis Research Foundation, 10675 John Jay Hopkins Drive, San Diego, CA 92121, USA*
[c]*Department of Lead Discovery, The Genomics Institute of the Novartis Research Foundation, 10675 John Jay Hopkins Drive, San Diego, CA 92121, USA*

Received 10 July 2006; revised 8 August 2006; accepted 9 August 2006
Available online 22 August 2006

Abstract—A series of PPARδ-selective agonists was investigated and optimized for a favorable in vivo pharmacokinetic profile. Isoxazole **LCI765** (**17d**) was found to be a potent and selective PPARδ agonist with good in vivo PK properties in mouse (C_{max} = 5.1 μM, $t_{1/2}$ = 3.1 h). **LCI765** regulated expression of genes involved in energy homeostasis in relevant tissues when dosed orally in C57BL6 mice. A co-crystal structure of compound **LCI765** and the LBD of PPARδ is discussed.

The peroxisome proliferator-activated receptors are ligand-activated transcription factors belonging to the nuclear hormone superfamily.[1,2] In recent years, the three distinct subtypes (PPARα, PPARγ, and PPARδ) have received great attention in both academic and pharmaceutical research due to their involvement in glucose and lipid homeostasis.[3–7]

In light of the success of the hypolipidemic fibrates and the TZD class of insulin sensitizers acting through activation of PPARα[1] and PPARγ,[8] respectively, pharmaceutical companies have focused efforts mostly on developing more potent and selective agonists on these two PPAR subtypes. More recent reports have raised the awareness for the third subtype, PPARδ, suggesting a likewise important role in energy homeostasis.[9,10] The synthetic PPARδ ligands used in these studies show significant cross-reactivity to other PPAR subtypes, which underscores the need for tool compounds with an improved PPARδ selectivity profile in order to distinguish the PPARδ-driven effects from those derived from activation of either PPARγ or/and PPARα subtypes.

We have recently described the identification of an isoxazole scaffold HTS hit and its optimization to the lead compound **1** (Fig. 1) with exceptional selectivity for PPARδ.[11] Unfortunately, all analogs in the series up to this point had shown rather poor bioavailability in mouse. Further optimization was necessary to solve the issue. Since neither replacement of the amide functionality in position 4 nor any change of substituent in position 5 led to an improvement in bioavailability, we focused our efforts on changing the core heterocycle and the head group substituent bearing the carboxylate in position 3.

Switching the nitrogen and oxygen of the isoxazole gave an 'inverted' isoxazole **2** with similar activities, but also similarly poor in vivo properties when compared to compound **1**. Changes from isoxazoles to any other heterocycles such as pyrazoles **3** and **4**, imidazoles **5**, and triazoles **6** were not tolerated and resulted in inactive analogs (Fig. 1).[12]

Keywords: Nuclear hormone receptor; PPAR agonist; PPARδ; Energy homeostasis; Metabolic xyndrome; Isoxazoles.
* Corresponding author. Tel.: +1 858 812 1720; fax: +1 858 812 1848; e-mail: repple@gnf.org

0960-894X/$ - see front matter © 2006 Elsevier Ltd. All rights reserved.
doi:10.1016/j.bmcl.2006.08.052

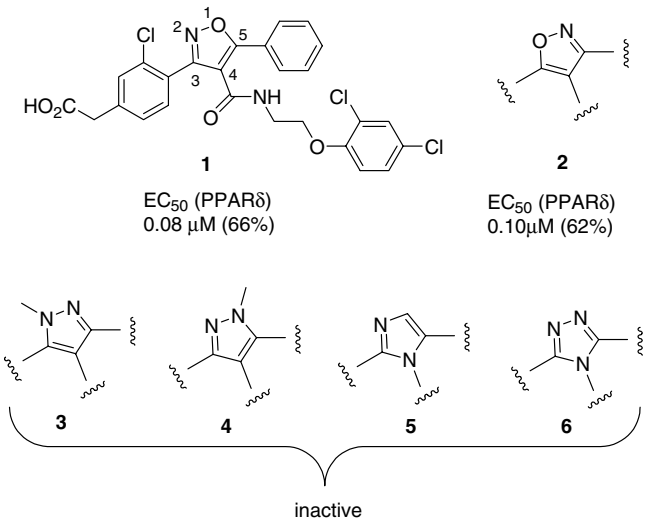

Figure 1. Changing the isoxazole core heterocycle led to loss of activity in all compounds except compound **2**.

Next, we directed our attention toward position 3 of the isoxazole. Most PPAR agonists connect the functional head group to the lipophilic tail group via a flexible linker. In our case, inserting a flexible linker between the head group and isoxazole core was accomplished by reacting 3-methyl-5-phenyl-isoxazole-4-carbonyl chloride **7** with *tert*-butanol (Scheme 1). The methyl group was brominated using NBS to give isoxazole **8**, followed by ether formation with the appropriate phenol or thiophenol **9**. Removal of the *tert*-butyl protecting group, activation of the acid with thionyl chloride, and amide formation with the amine **10** gave an intermediate ester, which was saponified to the final products **11**. Insertion of a flexible linker obliterated activity in all cases, which is exemplified in Table 1 by compound **11a.**

Since a direct single bond between head group phenyl and isoxazole is required for PPAR activation, we investigated changes in the head group phenyl substituents and/or their substitution patterns. Starting from the appropriate hydroxy-phenylacetic acids, hydroxy-phenylpropionic acids or hydroxy-phenoxyacetic acids **12** the carboxylate functionality was esterified, then the hydroxyl was triflated and converted to the cyanides **13** using zinc (II) cyanide (Scheme 2). Alternatively, when aromatic halides were available as starting materials instead of phenols, the triflation step could be omitted. Raney-nickel alloy reduction in formic acid, oxime formation, and chlorination gave the reactive chloroxime intermediates **14**. The cyclization partners **16** were synthesized by microwave-assisted amide formation from the corresponding β-ketoesters **15** with amine **10**, followed by deprotonation using potassium bis(trimethylsilyl)amide. The cyclization of intermediates **14** and **16** proceeded regioselectively under mild conditions, and saponification with lithium hydroxide gave the free carboxylates **17** in overall fair to good yields.

Table 1 shows a list of selected analogs and their in vitro activities in PPAR transactivation assays. All analogs presented were metabolically stable after incubation with mouse, rat, and human liver microsomes, and behaved similarly in a standard kinetic solubility assay. Based on an acceptable in vitro activity profile (EC_{50}-(PPARδ) < 100 nM), selected compounds were dosed in C57BL6 mice for an assessment of their in vivo pharmacokinetic properties. The mice were dosed po at 20 mpk in a 0.5% CMC suspension. The maximal concentration (C_{max}) and half-life ($t_{1/2}$) were calculated from a 24 h time course study.

All analogs disclosed in the first publication[11] were rapidly cleared when dosed iv, regardless of the nature of the substituents in positions 4 and 5 of the isoxazoles. This was also reflected in their low C_{max} (<0.3 μM) and short half-lives (<0.5 h) when dosed po, exemplified by compound **1** in Table 1. Notably, these compounds

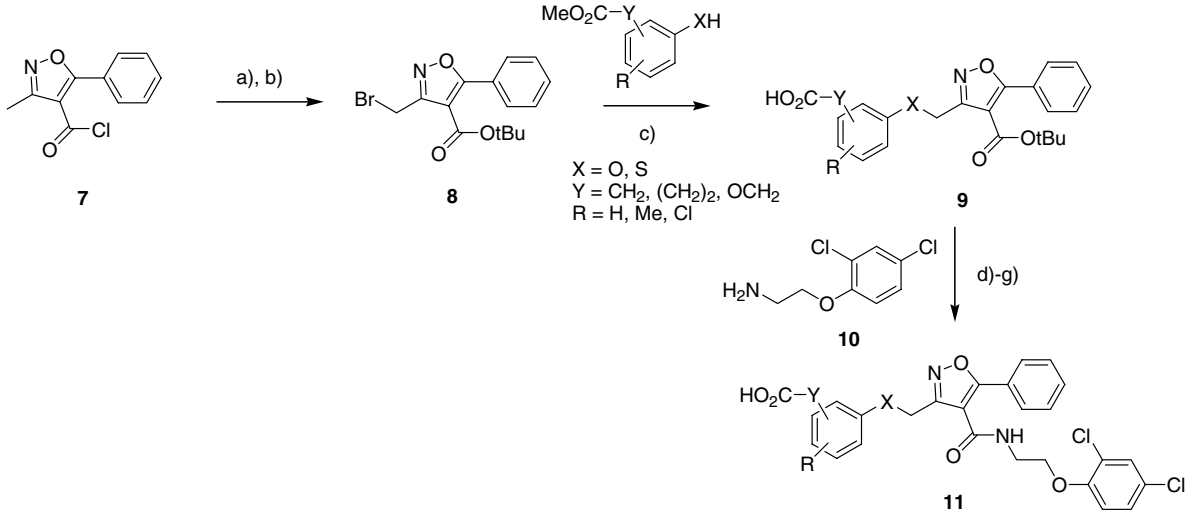

Scheme 1. Reagents and conditions: (a) *t*-BuOH, pyridine, DCM, rt, 12 h (70%); (b) NBS, CCl_4, rt, 12 h (43%); (c) Cs_2CO_3, CH_3CN, rt, 2 h (>90%); (d) TFA/DCM 1:5, rt, 7 h (>90%); (e) $SOCl_2$, benzene, 80 °C, 2 h (80–90%); (f) compound **10**, K_2CO_3, DCM, rt, 12 h (>80%); (g) 1 N LiOH, THF, rt, 12 h (95%).

Table 1. In vitro transactivation and in vivo pharmacokinetic properties of selected examples

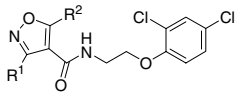

Compound	R^1	R^2	Cell-based transactivation[a]			In vivo PK (mouse) 20 mpk po	
			huPP ARα EC_{50} (μM)	huPP ARγ EC_{50} (μM)	huPP ARδ EC_{50} (μM)[a]/% eff	C_{max} (μM)	$t_{1/2}$ (h)
1	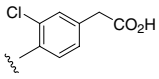		>10	>10	0.08/66%	<0.3	<0.5
11a	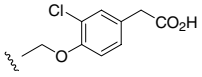		>10	>10	>10		
17a	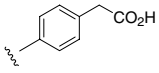		>10	>10	0.72/42%		
17b	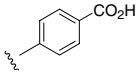		>10	>10	>10		
17c	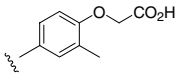		>10	>10	0.20/60%	<0.3	<0.5
17d	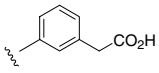		>10	>10	0.07/83%	5.1	3.1
17e	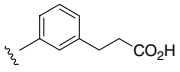		>10	>10	0.97/38%		
17f	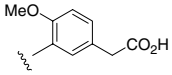		>10	>10	0.56/70%		
17g	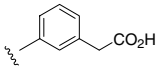		>10	>10	1.07/52%		
17h	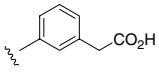		>10	>10	0.09/65%	<0.3	<0.5
17i	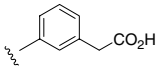		>10	>10	0.05/76%	1.9	1.5
17j	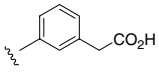		>10	>10	0.06/83%	5.6	1.1

[a] Concentration of test compound that produced 50% of the maximal reporter activity (100% control: GW501516); all data within ±25%.

shared a *para* substituted 3-chloro-phenylacetic acid in position 3 of the isoxazole (R^1).

Removing the chloride (compound **17a**) led to an approximately 10-fold reduction in activity. Switching from phenylacetic acids to benzoic acid analogs obliterated activity, regardless of the carboxylate being in *ortho*, *meta* or *para* (compound **17b**) position. On the other hand, extending the carboxylate substituent to phenyl propionic acids or phenoxyacetic acids (exemplified by compound **17c**) retained activity, but did not lead to an improvement of the in vivo PK profile.

A breakthrough was achieved when the *para* substitution pattern of the phenylacetic acid (compound **17a**) was changed to *meta* (compound **17d**, **LCI765**). Compound **LCI765** not only displayed good in vitro activity and selectivity for the PPARδ subtype, but also showed a tremendous improvement in its in vivo PK profile (C_{max} = 5.1 μM, $t_{1/2}$ = 3.1 h). **LCI765** was tested in vivo in an acute dosing study in C57BL6 mice.[13] Similar to the PPARδ-selective ligand GW501516,[14–16] LCI765 regulated expression of genes involved in glucose and lipid metabolism (PDK4 and ApoAIV), and energy uncoupling (UCP3) in skeletal muscle and intestinal tissues (Fig. 2).

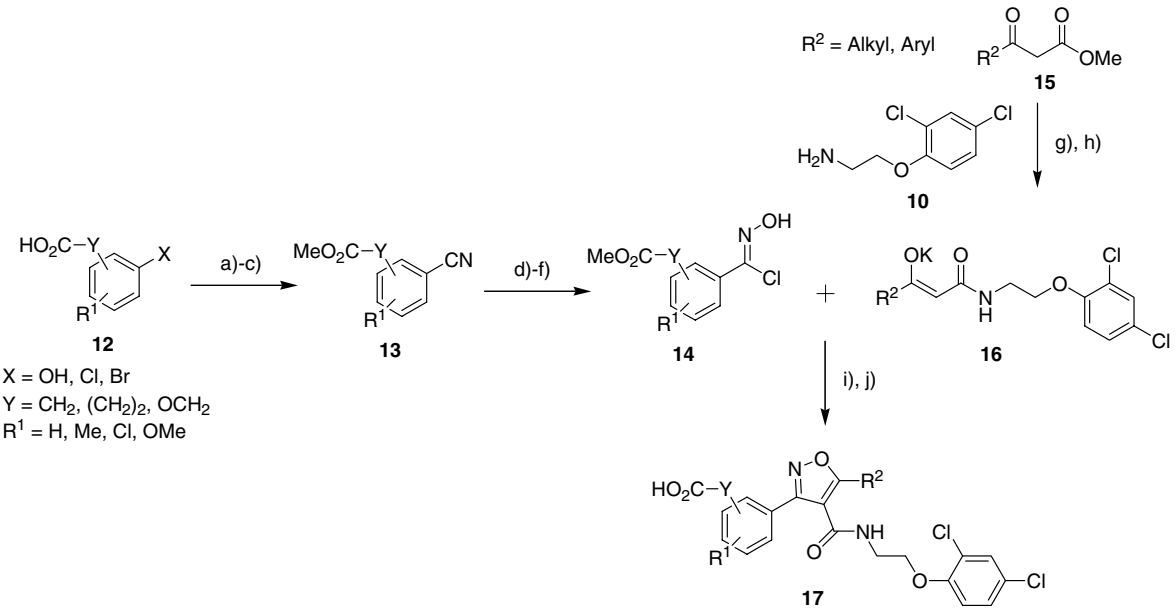

Scheme 2. Reagents and conditions: (a) MeOH, H_2SO_4, reflux, 8 h, quant.; (b) Tf_2O, NEt_3, DCM, 0 °C, 1 h (>95%); (c) $Zn(CN)_2$, $Pd(PPh_3)_4$, DMF, 80 °C, 30 h (60–80%); (d) Raney-alloy, H_2CO_2, 110 °C, 10 h (50–60%); (e) $H_2NOH{\cdot}HCl$, Na_2CO_3, H_2O, rt, 2 h, (>90%); (f) NCS, DMF, HCl(g), rt, 30 min; (g) compound **10**, toluene, MW (160 °C, 10 min) (40–60%); (h) $KN(TMS)_2$, Et_2O, rt, 1 h; (i) CH_3CN, rt, 3 h (60–80%); (j) 1 N LiOH, THF, rt, 12 h (>95%).

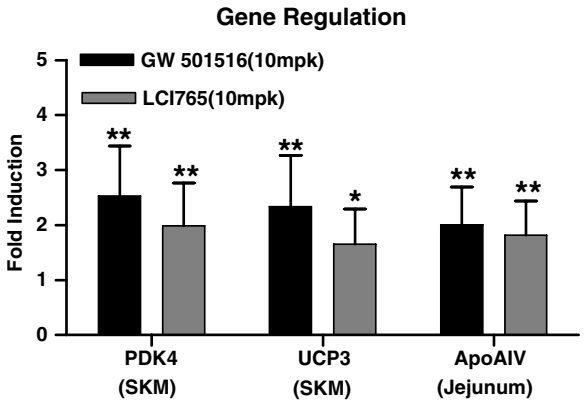

Figure 2. Acute dosing-induced gene assay of **LCI765**. Tissues were harvested from C57BL/6 mice dosed for 3 days with vehicle, GW501516 or **LCI765**. The expression of various genes was analyzed by real-time PCR analysis. Fold induction is reported relative to vehicle control. *p value < 0.03, **p value < 0.01.

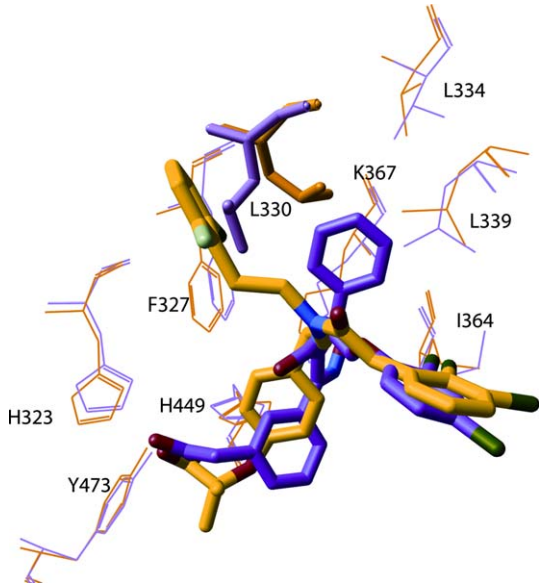

Figure 3. Superposition of co-crystal structures of the PPARδ LBD with **LCI765** (blue) and GW2433 (yellow). The image was generated using Maestro GUI (Schrodinger, Inc.).

Extension of the carboxylate substituent (compound **17e**) or additional substituents (cf. compound **17f**) did not lead to improved in vitro activities. Changes of the amide substituent in position 4 of the isoxazole core were not well tolerated, following the trend of narrow SAR described in the earlier communication.[11] In general, alkyl substituents in position 5 (R_2) (e.g., compound **17g**) had deleterious effects on PPARδ in vitro activity. Small heterocycles as in compound **17h** were tolerated, but lacked favorable PK. The only other active and bioavailable compounds in addition to the plain phenyl substituted analog **LCI765** displayed an *ortho* substituted phenyl ring as in compounds **17i** and **17j**.

LCI765 was co-crystallized with the ligand binding domain (LBD) of PPARδ (Fig. 3).[17] The root mean square deviation of backbone atoms between residues in the LBD (29 residues) of our crystal structure and the equivalent residues in the co-crystal structure of PPARδ/GW2433 (pdb code 1GWX[18]) is ~0.7 Å, indicating a very similar overall conformation. The orientation of head group and tailgroup is in accordance with the docking results of the original HTS hit used in the design of the isoxazole series.[11] However, the model would fail to predict the tolerance of large substituents in position 5 of the isoxazole. The most prominent conformational change from the PPARδ/GW2433 structure used

in the docking study to the co-crystal structure with **LCI765** is observed for the dihedral angle chi-1 of Leu330, whose value is different by ~100°.[19] This movement is necessary in order to enlarge a cavity lined by residues Phe327, Leu330, Val334, Leu339, Ile364, and Lys367, so that it can accommodate the phenyl ring in position 5 of the isoxazole. The corresponding cavity does not exist in PPARα and PPARγ where both isoforms have the bigger Met residues in place of Val334 and Ile364, respectively. This might explain the observed PPARδ selectivity of 3,4,5-trisubstituted isoxazoles.

In summary, PPARδ-selective isoxazoles **17d**, **17i**, and **17j** exhibiting greatly improved mouse in vivo pharmacokinetic properties were identified, while the in vitro activity and selectivity of the three isoxazoles was maintained or improved compared to compound **1**. This was achieved by optimization of the head group in position 3 of the isoxazole core of compound **1**. Compound **LCI765** (**17d**) regulates expression of genes involved in energy homeostasis in relevant tissues when dosed orally in C57BL6 mice. Additionally, a co-crystal structure of compound **LCI765** with the PPARδ ligand binding domain revealed the formation and occupancy of a new hydrophobic cavity. This cavity may be formed exclusively in the PPARδ isoform due to the smaller amino acid side chains lining the pocket as compared to the other isoforms. Compound **LCI765** represents the first example to occupy this side pocket and underlines the flexibility of the PPAR ligand binding domain to accommodate various diet-derived lipids and their metabolites. **LCI765** should be a useful tool compound to elucidate the pharmacological consequences of selective PPARδ activation.

Acknowledgments

We gratefully acknowledge Drs. T. R. Vedananda, Sandra Teixeira, and Peter G. Schultz for their helpful discussions and support. We also thank ActiveSight, San Diego, for their support in our co-crystallization efforts.

Supplementary data

Supplementary data associated with this article can be found, in the online version, at doi:10.1016/j.bmcl.2006.08.052

References and notes

1. Issemann, I.; Green, S. *Nature* **1990**, *347*, 645.
2. Mangelsdorf, D. J.; Evans, R. M. *Cell* **1995**, *83*, 841.
3. Cheng, P. T. W.; Mukherjee, R. *Mini-Rev. Med. Chem.* **2005**, *5*, 741.
4. Staels, B.; Fruchart, J.-C. *Diabetes* **2005**, *54*, 2460.
5. Evans, R. M.; Barish, G. D.; Wang, Y.-X. *Nat. Med.* **2004**, *10*, 355.
6. Berger, J.; Moller, D. E. *Annu. Rev. Med.* **2002**, *53*, 409.
7. Willson, T. M.; Brown, P. J.; Sternbach, D. D.; Henke, B. R. *J. Med. Chem.* **2000**, *43*, 527.
8. Willson, T. M.; Cobb, J. E.; Cowan, D. J.; Wiethe, R. W.; Correa, I. D.; Prakash, S. R.; Beck, K. D.; Moore, L. B.; Kliewer, S. A.; Lehmann, J. M. *J. Med. Chem.* **1996**, *39*, 665.
9. Leibowitz, M. D.; Fievet, C.; Hennuyer, N.; Peinado-Onsurbe, J.; Duez, H.; Berger, J.; Cullinan, C. A.; Sparrow, C. P.; Baffic, J.; Berger, G. D.; Santini, C.; Marquis, R. W.; Tolman, R. L.; Smith, R. G.; Moller, D. E.; Auwerx, J. *FEBS Lett.* **2000**, *473*, 333.
10. Oliver, W. R., Jr.; Shenk, J. L.; Snaith, M. R.; Russell, C. S.; Plunket, K. D.; Bodkin, N. L.; Lewis, M. C.; Winegar, D. A.; Sznaidman, M. L.; Lambert, M. H.; Xu, H. E.; Sternbach, D. D.; Kliewer, S. A.; Hansen, B. C.; Willson, T. M. *Proc. Natl. Acad. Sci. U.S.A.* **2001**, *98*, 5306.
11. Epple, R.; Russo, R.; Azimioara, M.; Cow, C.; Xie, Y.; Wang, X.; Wityak, J.; Karanewsky, D.; Gerken, A.; Iskandar, M.; Saez, E.; Seidel, H. M.; Tian, S.-S. *Bioorg. Med. Chem. Lett.* **2006**, *16*, 4376.
12. The synthetic procedures of all analogs described in this communication except compounds **3**–**6** and **11a** can be found in the following patent application: Epple, R.; Russo, R.; Azimioara, M.; Xie, Y. WO 2005113519. Synthetic procedures of compounds **3**–**6** and **11a** can be found in the supplementary material.
13. C57BL/6 male mice (age 8–9 weeks, Charles River Laboratories) were orally gavaged once daily with the compounds at 10 mg/kg or with vehicle (0.5% CMC: 2% Tween 80) for 3 days. On the 4th day and 4 h after the last dose was administered, mice were euthanized. Samples of skeletal muscle (quadriceps), adipose tissue, jejunum, and ileum were collected, rapidly frozen in liquid nitrogen, and stored at −80 °C. Total RNA was isolated from the tissues and SYBR Green quantitative real-time-PCR was performed on an ABI PRISM 7900HT Sequence Detection system (Applied biosystems). For each sample, the quantity of the target gene and the endogenous reference GAPDH was determined to obtain a normalized target value. Data were analyzed using SDS 2.0 software (Applied biosystems).
14. Dressel, U.; Allen, T. L.; Pippal, J. B.; Rohde, P. R.; Lau, P.; Muscat, G. E. O. *Mol. Endocrinol.* **2003**, *17*, 2477.
15. Wang, Y.-X.; Lee, C.-H.; Tiep, S.; Yu, R. T.; Ham, J.; Kang, H.; Evans, R. M. *Cell* **2003**, *113*, 159.
16. Tanaka, T.; Yamamoto, J.; Iwasaki, S.; Asaba, H.; Ikeda, Y.; Watanabe, Y.; Uchiyama, Y.; Sumi, K.; Iguchi, H.; Ito, S.; Doi, T.; Hamakubo, T.; Naito, M.; Auwerx, J.; Yanagisawa, M.; Kodama, T.; Sakai, J. *Proc. Natl. Acad. Sci. U.S.A.* **2003**, *100*, 15924.
17. Atomic coordinates of the co-crystal structure have been deposited with the PDB and are accessible under the code 2J14.
18. Xu, H. E.; Lambert, M. H.; Montana, V. G.; Parks, D. J.; Blanchard, S. G.; Brown, P. J.; Sternbach, D. D.; Lehmann, J. M.; Wisely, G. B.; Willson, T. M.; Kliewer, S. A.; Milburn, M. V. *Mol. Cell* **1999**, *3*, 397.
19. The amino acid labels in Figure 3 are given in consistency with published crystal structures, but do not correspond to actual PPARδ sequence numbering. The actual numbers for residues Phe327, Leu330, Val334, Leu339, Ile364, and Lys367 are Phe291, Leu294, Val298, Leu303, Ile328, and Lys331, respectively.